Depth Profiling of Melting and Metallization in Si(111) and Si(001) Surfaces

R. Gunnella,[1] M. Ali,[1,*] M. Abbas,[1,†] F. D'Amico,[2,1] E. Principi,[2,1] and A. Di Cicco[1,‡]

[1]CNISM, Sezione Fisica, Scuola di Scienze e Tecnologie, Università di Camerino, via Madonna delle Carceri, I-62032 Camerino (MC), Italy

[2]Synchrotron ELETTRA, Strada Statale 14 - I-34149 Basovizza, Trieste, Italy

(Received 9 February 2011; published 14 October 2011)

An original approach for measuring the depth profile of melting and metallization of the Si(111) and Si(001) surfaces is proposed and applied. The different probing depths of the Auger electron and electron energy loss (EELS) spectroscopies are exploited to study the number of molten and metallic layers within 5–30 Å from the surface up to about 1650 K. Melting is limited to 3 atomic layers in Si(001) in the range 1400–1650 K while the number of molten layers grows much faster (5 layers at about 1500 K) in Si(111) as also indicated by the L_3-edge shift observed by EELS. The relationship between melting and metallization is briefly discussed.

DOI: 10.1103/PhysRevLett.107.166103 PACS numbers: 68.35.Rh, 64.70.D−, 73.20.−r, 79.20.Fv

Surface melting has been studied for a long time in view of the importance of this phenomenon in understanding basic questions related to first-order phase transitions in solids (see [1,2] and references therein). A starting point motivating a microscopic study of surface melting is the fact that undercooled liquids can be obtained rather easily while overheating a solid is extremely difficult. In fact, this is explained by the existence of a wet surface well below the melting point, providing the initial germ for melting. The general interest of this phenomenon is epitomized by the ice premelting literature [3], but scattered experimental studies deal with microscopic details of the surface melting processes under high-temperature conditions (see, for example, [4–10]). After the initial detailed study on the crystal-face dependence of Pb surface melting [4,5], very little experimental information was obtained about the number of disordered atomic layers approaching the bulk melting temperature. Another important effect, still lacking a clear connection with surface melting, is the surface metallization observed in many semiconductors well below the melting temperature [9,11,12].

In pure semiconductors like silicon, several questions about the behavior of the surface at high temperatures are still open. Incomplete melting of the first two layers has been observed in Si(001) by photoelectron diffraction [7], later discussed also by other authors (see, for example, [8,10,13]) using different techniques, above about 1400 K. Metallization of the Si(001) surface was observed to occur at much lower temperatures between 900 and 1200 K [12,13]. The Si(111) surface behaves differently; in fact, it shows a transition between the 7×7 and 1×1 reconstruction completed around 1140 K. At higher temperatures, the top bilayer was found to become disordered [9,14,15] around 1470 K. Moreover, recent *ex situ* atomic force microscopy images of Si(111) surfaces [16] showed structures assigned to "premelting" of about 3 bilayers (about 9 Å) around 1500 K.

Stimulated by the need to shed some light on this complex scenario, we tackled the problem of a systematic study of surface melting and metallization of the Si(001) and Si(111) surfaces. In this Letter, we present a detailed investigation of those transitions using Si LVV, Si KLL Auger electron (AES), and $L_{2,3}$ electron energy loss (EELS) spectroscopies. For this purpose, we have taken advantage and improved the performances of high-temperature UHV experiments under controlled conditions [17–19]. The different probing depths of these surface-sensitive techniques are exploited to study the increase in the number of molten and metallic layers within 5–30 Å from the surface up to temperatures of about 1650 K.

Samples were obtained by Si(111) and Si(001) wafers (B p doped), cleaned and characterized using standard procedures for surface science. High-temperature AES and EELS experiments were performed in an UHV chamber using a cylindrical mirror analyzer with a coaxial electron gun. Low-noise high-temperature measurements were performed using a special Ta crucible ensuring homogeneous heating and temperature control of the sample surfaces, while temperatures were measured with an optical pyrometer (~ 1 mm spot size) and calibrated within 10 K [17–19].

In Fig. 1 we report, from the top to the bottom, the main results of our extended set of high-temperature LVV, KLL Auger and EELS experiments. The peak-to-peak intensity (amplitude of the first derivative signal) of the LVV Auger emission line (92 eV) is shown as a function of temperature in the upper panel for the Si(111) and Si(001) surfaces, respectively. In Fig. 1, middle panel, we report the temperature trend of the peak-to-peak intensity of the KLL Auger emission line (1614 eV) for the two surfaces. In the lower part of Fig. 1 we report the energy shift observed for the Si $2p$ edge EELS spectra (kinetic energies of ~400 eV).

The surface sensitivity of these three sets of experiments is very different, due to the known escape depth variation

 © 2011 American Physical Society

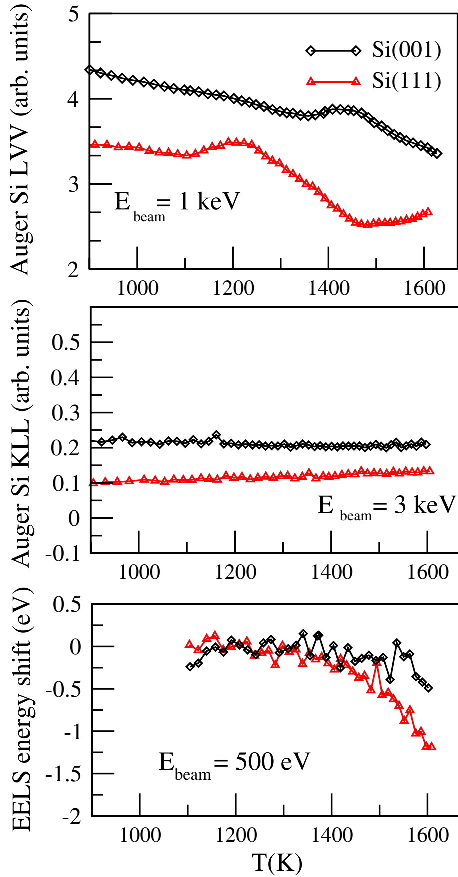

FIG. 1 (color online). Upper panel: Auger Si *LVV* signals of the Si(111) and Si(001) surfaces up to about 1600 K. Middle panel: Auger Si *KLL* signals in the same temperature range. Lower panel: Edge energy shift of the Si $L_{2,3}$ energy loss spectra (EELS) associated with the two surfaces. The incident beam energies (E_{beam}) are reported in each panel.

with kinetic energy. *LVV*, EELS, and *KLL* data probe atomic layers within about 5, 12, and 35 Å from the surface, respectively [20]. In Fig. 1 (upper panel) we can see that distinct features are visible around 1200 and 1400 K for the Si(111) and Si(001) *LVV* intensity. These features cannot be found in the *KLL* intensity trend (middle panel) and are clearly associated with surface transitions involving few atomic layers. The absence of visible changes in the *KLL* Auger intensity up to ~1600 K indicates that a negligible fraction of the probed atomic layers, within about 35 Å, is involved in phase transitions. The edge energy shift probed by EELS (lower panel of Fig. 1) reflects the increase of the electron density of states within the energy gap (around 1.1 eV), also for excitations beyond the dipole approximation. The shift shows a continuous trend which is interpreted as mainly due to the metallization of successive atomic layers as a function of temperature within the ~12 Å probing depth. The known thermal dependence of the energy gap has been removed as a linear contribution in the investigated range of temperature [21].

The features observed in the *LVV* intensity are consistent with surface transitions described in the literature. In fact, He ions scattering data [14] indicate an order-order transition (7×7 to 1×1) occurring between 1140 and 1200 K for the (111) surface, while anomalies at 1400 K for the (001) surface are rather associated with disorder effects due to the formation of a liquid double layer.

The *LVV* data shown in Fig. 1 can be analyzed taking into account that the variation in the intensity of the Auger signal is affected by interference effects of the incident and outgoing beams within the lattice [22], depending on the geometry of the experiment and on the relative orientation of the surface. In this way, the AES intensity is dependent on thermal and structural disorder within the probed depth [22,23]. In the experiment under consideration (normal incidence for the ingoing electrons of the electron gun and azimuth average of the outgoing electrons), we expect that the Auger intensity is strongly affected by the ordering of collinear atomic configurations normal to the surface (focusing effect), as it is the case for the high-temperature reconstructions of the Si(111) and Si(001) surfaces. The features associated with an increase of the *LVV* intensity trends are interpreted as the onset of those transitions, and the increase itself can possibly be related to a denser atomic structure of the first surface layers. At higher temperatures, above 1200 and 1400 K for Si(111) and Si(001), respectively, an increased attenuation rate of the *LVV* intensity is observed. The intensity decay for increasing temperature can be explained by an increasing thermal disorder in the atomic positions, which is different according to the nature of the surface phase. Because of the very limited electron escape depth λ, the *LVV* peak-to-peak intensity I shown in Fig. 1 is due mainly to few uppermost layers. For this reason, we have used a simple expression [22] for the intensity I at a given temperature T:

$$I(T) = I_0 \sum_i e^{-z_i/\lambda - q^2 \rho_i^2(T)}, \tag{1}$$

where the sum is extended over the first four atomic layers, z_i is the depth of the ith atomic layer, and q is the electron momentum. A simple Einstein model is used for the mean-square displacement associated with the atoms of the atomic layer i:

$$\rho_i^2 = 1/3\langle u_{E,i}^2 \rangle = \frac{\hbar^2}{(2Mk_B\theta_i)} \coth(\theta_i/2T) \tag{2}$$

expressed in terms of the Einstein temperatures θ_i and the silicon atomic weight M [24].

The best-fit values for the Einstein temperatures θ_i approach the limit for bulk silicon ($T_E \sim 520$ K) for the inner layers at moderate temperatures. The results of the fitting of the intensity decay at high temperatures using Eqs. (1) and (2) are shown in Fig. 2 in terms of the Lindemann ratio $C_L = \frac{\rho_i}{R}$ (R being the average first-neighbor interatomic distance), commonly used as a

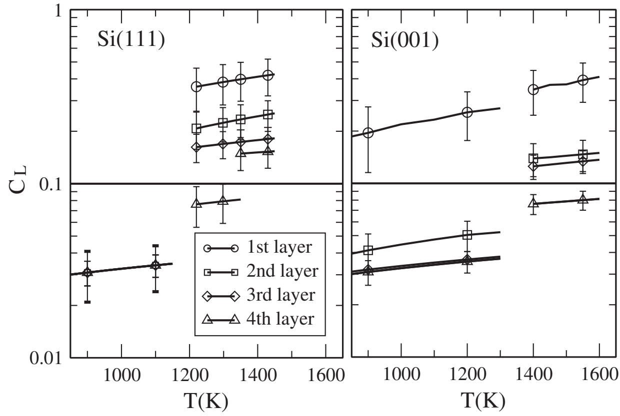

FIG. 2. Fractional mean-square vibrational amplitude (Lindemann ratio C_L) as a function of temperature as obtained through a layer by layer analysis (see text) of Auger LVV data. Significant differences are obtained for the Si(111) (left panel) and Si(001) (right panel) surfaces.

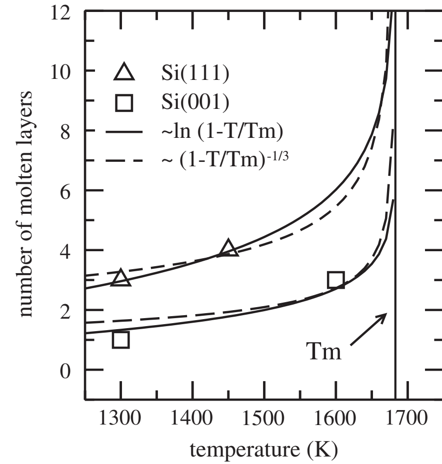

FIG. 3. Number of molten layers for the Si(111) (triangles) and Si(001) (squares) surfaces as a function of temperature. A power law (continuous lines) and a logarithmic trend (dashed lines) obtained by realistic surface melting models are compared with present data (empty symbols).

fingerprint for melting when C_L is greater than 10% [25]. A very different behavior is found for the two surfaces Si (111) and Si(001) as a function of temperature (the 1st and the 4th layers in Fig. 2 are the topmost and the deepest surface layers, respectively). These results are also confirmed using a simple parametrization of the layer Einstein temperatures θ_i through a monotonic function of the depth z_i (asymptotic bulk T_E reached for the inner layers).

In Si(111), an abrupt change of the mean-square displacements of the four probed atomic layers is observed above 1200 K, compatible with melting of those near-to-surface layers. The change of slope in the LVV intensity around 1300 K and the fairly constant LVV intensity observed above 1450 K (see Fig. 1) are a clear indication that the two uppermost bilayers are finally melted and that the Si(111) surface melting proceeds within the bulk beyond the depth probed by the Auger electrons (~ 5 Å).

In Si(001), LVV data are consistent with lateral disordering of the uppermost atomic layer already at 800 K and with melting of the first three atomic layers above 1400 K. No saturation of the LVV decay is observed, suggesting that the surface melting is limited to the first surface layers up to 1600 K.

The thickness of the molten surface as a function of the temperature can be estimated using a power $(T - T_m^{\text{bulk}})^{-1/3}$ [2] or a logarithmic $-\ln(1 - T/T_m)$ model (see Refs. [1,2] and references therein). The different behavior near the melting point depends on the nature of the interatomic forces, resulting in a power-law divergence when dominated by long-range interactions or in a logarithmic one for short-range forces. The number of molten layers for increasing temperature measured in this work is compared with the trend of those models in Fig. 3. The LVV data do not allow us to select between the two laws, although the log model better reproduces both the Si(111) and Si(001) data. For the Si(111) surface, the first three layers (~ 4.4 Å) are already liquid according to the Lindemann criterion above 1200 K, and four layers (those probed by LVV Auger electrons) are molten above 1400 K (triangles in Fig. 3). Both curves corresponding to the power-law and log models in Fig. 3 show a rather marked increase of the number of molten layers approaching the melting point (about 5 atomic layers molten at 1600 K, more than 80 K before T_m). In contrast to the Si(111) case, the Si(001) surface exhibits an incomplete melting, because the melting process is frozen to three layers up to about 1650 K (see Fig. 3). These results can possibly be rationalized in light of the previous observations and calculations showing that enhanced vibrations for specific surface geometries [26], as well as a poorer surface packing and first-neighbor bonding and coordination [1,5], favor surface melting. In our case, the backbonds nearly parallel to the surface Si(111) are able to induce surface premelting through large anisotropic vibrations, as also observed for other surfaces including ice (see Ref. [26]).

The observed metallization of the surface layers probed by EELS (see Fig. 1, lower panel) follows the trend observed using AES. EELS edge shifts corresponding to about 1 and 0.4 eV at 1600 K, for Si(111) and Si(001), respectively, are interpreted as due to the closure of the gap [17] induced by disordering or melting of the successive layers. Those data can be used to measure the depth profile of the metal to semiconductor interface, using a simple model based on the edge shift due to a metallic layer weighted according to the ratio between the layer distance from the surface and the probing depth.

The results of the depth profiling of melting and metallization at the two surfaces Si(111) and Si(001) are reported in Fig. 4. For the Si(001) surface (left panel in Fig. 4) the observed increase in the number of molten layers

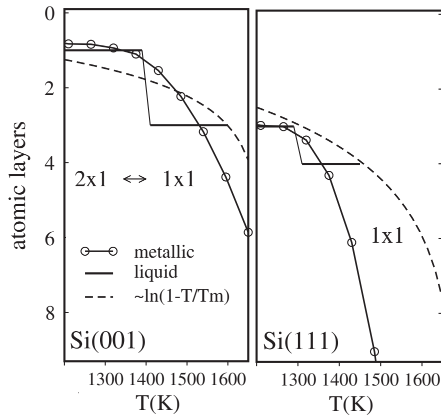

FIG. 4. Penetration of molten and metallic layers as a function of temperature for Si(001) (left) and Si(111) (right) surfaces. The number of metallic layers measured by EELS (lines with empty circles) is compared with the trend of molten layers (*LVV* data analysis, continuous lines; log model, dashed lines).

accompanies the surface transition observed around 1400 K and previously assigned to incomplete surface melting [7] and/or to a (2×1) to (1×1) ideal surface termination [10,27]. The number of atomic layers corresponding to metallic electron states increases gradually with temperature reaching about 4 layers at 1600 K. On the other hand, both molten and metallic layers proceed much faster for the Si(111) surface, reaching 6 molten layers at 1600 K and much greater than 10 with metallic character (see right panel in Fig. 4).

These results show that while molten layers near the surface always have metallic nature, the interface metal-semiconductor is extended to deeper layers for increasing temperature. We can speculate observing that this appears reasonable in light of the band-bending mechanism characteristic of metal-semiconductor interfaces and of the natural extension of the electron states inside the gap [28,29]. The comparison between the solid-liquid and the metal-semiconductor interface, shown here for the first time, certainly deserves further investigation. In conclusion, we have shown in this work, using the same experimental techniques, that surface melting is limited to 3 atomic layers in Si(001) in the entire range (1400–1650 K) while the number of molten layers grows much faster (5 layers at about 1500 K) in Si(111). Those results can possibly be related to the large vibrational amplitudes of outermost atoms at the Si(111) surface [26]. The present results can be directly compared with computer simulations of surface melting and stimulate further studies of disordering and metallization of surfaces.

Supplemental Material about experimental and data-analysis methods presented in this work can be found in Ref. [30].

This work has been carried out in the framework of the TIMEX project [31]. E. P. and M. Abbas gratefully acknowledge postdoctoral grants.

*Present address: Department of Physics, COMSATS Institute of Information Technology, Park Road, Chak Shahzad, Islamabad, 44000, Pakistan.
†Present address: LIOS, Johannes Kepler University Linz, Alltenberger Strasse 69, A-4040 Linz, Austria.
‡Also at: IMPMC, Université Paris 6, CNRS, Campus Jussieu, 4 place Jussieu, 75005 Paris, France.

[1] U. Tartaglino, T. Zykova-Timan, F. Ercolessi, and E. Tosatti, Phys. Rep. **411**, 291 (2005).
[2] A. Trayanov and E. Tosatti, Phys. Rev. Lett. **59**, 2207 (1987).
[3] J. G. Dash, A. W. Rempel, and J. S. Wettlaufer, Rev. Mod. Phys. **78**, 695 (2006).
[4] J. W. M. Frenken, P. M. J. Marée, and J. F. van der Veen, Phys. Rev. B **34**, 7506 (1986).
[5] B. Pluis, A. W. Denier van der Gon, J. W. M. Frenken, and J. F. van der Veen, Phys. Rev. Lett. **59**, 2678 (1987).
[6] P. Carnevali, F. Ercolessi, and E. Tosatti, Phys. Rev. B **36**, 6701 (1987).
[7] J. Fraxedas, S. Ferrer, and F. Comin, Europhys. Lett. **25**, 119 (1994).
[8] M. Kimura and A. Ikari, J. Appl. Phys. **89**, 2138 (2001).
[9] Y. Fukaya and Y. Shigeta, Phys. Rev. B **65**, 195415 (2002).
[10] Y. Fukaya and Y. Shigeta, Phys. Rev. Lett. **91**, 126103 (2003).
[11] S. Modesti, V. R. Dhanak, M. Sancrotti, A. Santoni, B. N. J. Persson, and E. Tosatti, Phys. Rev. Lett. **73**, 1951 (1994).
[12] L. Gavioli, M. G. Betti, and C. Mariani, Phys. Rev. Lett. **77**, 3869 (1996).
[13] A. Santoni, V. R. Dhanak, L. Grill, and L. Petaccia, Surf. Sci. **474**, L217 (2001).
[14] G. Lange, C. A. Meli, J. P. Toennies, and E. F. Greene, Phys. Rev. B **56**, 4642 (1997).
[15] Y. Fukaya and Y. Shigeta, Phys. Rev. Lett. **85**, 5150 (2000).
[16] V. Ignatescu and J. M. Blakely, Surf. Sci. **601**, 5459 (2007).
[17] A. Di Cicco, B. Giovenali, R. Gunnella, and E. Principi, Solid State Commun. **134**, 577 (2005).
[18] A. Di Cicco, B. Giovenali, R. Bernardini, and E. Principi, Phys. Scr. **T115**, 1068 (2005).
[19] A. Di Cicco, R. Gunnella, R. Marassi, M. Minicucci, R. Natali, G. Pratesi, E. Principi, and S. Stizza, J. Non-Cryst. Solids **352**, 4155 (2006).
[20] C. J. Powell and A. Jablonski, J. Phys. Chem. Ref. Data **28**, 19 (1999).
[21] V. Alex, S. Finkbeiner, and J. Weber, J. Appl. Phys. **79**, 6943 (1996).
[22] Y. Gao and J. Cao, Phys. Rev. B **43**, 9692 (1991).
[23] D. Sebilleau, R. Gunnella, Z.-Y. Wu, S. D. Matteo, and C. R. Natoli, J. Phys. Condens. Matter **18**, R175 (2006).
[24] M. Hasegawa, M. Watabe, and K. Hoshino, J. Phys. F **10**, 619 (1980).
[25] G. Grimvall and S. Sjödin, Phys. Scr. **10**, 340 (1974).
[26] M. A. Van Hove, J. Phys. Chem. B **108**, 14265 (2004).
[27] K. Sumitomo, H. Hibino, Y. Homma, and T. Ogino, Jpn. J. Appl. Phys. **39**, 4421 (2000).
[28] V. Heine, Phys. Rev. **138**, A1689 (1965).
[29] A. Cros and P. Muret, Mater. Sci. Rep. **8**, 271 (1992).
[30] See Supplemental Material at http://link.aps.org/supplemental/10.1103/PhysRevLett.107.166103 for information about experimental and data-analysis methods.
[31] http://gnxas.unicam.it/TIMEX